

## *In Situ* Cross-Linking of Electrospun Poly(vinyl alcohol) Nanofibers

Christina Tang, Carl D. Saquing, Jonathon R. Harding, and Saad A. Khan\*

Department of Chemical and Biomolecular Engineering, North Carolina State University, Raleigh, North Carolina 27695-7905

Received October 12, 2009; Revised Manuscript Received December 4, 2009

**ABSTRACT:** We examine single step reactive electrospinning of poly(vinyl alcohol) (PVA) and a chemical cross-linking agent, glutaraldehyde (GA), with hydrochloric acid (HCl) as a catalyst to generate water insoluble PVA nanofibers. Such an approach using a conventional setup with no modification enables the fibers to cross-link during the electrospinning process, thereby eliminating the need for post-treatment. Significant changes in the rheological properties occur during *in situ* cross-linking, which we correlate with electrospinnability. In particular, we associate changes in dynamic rheological properties to changes in fiber morphology for two regions: (1) below the critical concentration to electrospin PVA only and (2) above the critical concentration to electrospin PVA only. In region 1 fiber morphology changes from beaded fibers to uniform fibers to flat fibers, and in region 2 fiber morphology changes from uniform fibers to flat fibers. Electrospinning windows to generate uniform fibers for both regions are determined and can be manipulated by changing the molar ratio of GA to PVA and the volume ratio of HCl to GA. The electrospun fibrous material generated can be rendered insoluble in water, and the uniform fiber morphology can be maintained after soaking in water overnight. The reactive electrospinning process also lowers the critical PVA concentration required for successful electrospinning of the system.

### Introduction

Poly(vinyl alcohol) (PVA) is a water-soluble and biocompatible polymer, with excellent chemical and thermal stability.<sup>1,2</sup> Applications of PVA are limited by its hydrophilicity, but chemical cross-linking improves its stability in aqueous media.<sup>3,4</sup> Chemical cross-linking by glutaraldehyde (GA), a dialdehyde, during which the hydroxyl groups of the PVA and the aldehyde groups of GA react in the presence of a strong acid, has been well studied.<sup>4–7</sup> Membranes of nanofibrous cross-linked PVA are being studied in filtration and membrane applications. Cross-linking is advantageous because it renders the nanofibers insoluble in all solvents and increases the mechanical properties of the membranes; insolubility is especially desirable for filtration applications.<sup>2–4,6,8</sup>

Electrospinning is a simple technique used to generate nanofibrous membranes and nanofiber composites.<sup>9–16</sup> It involves the application of a high voltage (1–30 kV) to induce the formation of a liquid jet of polymer solution or melt. As the jet of polymer solution is stretched and whipped due to electrostatic forces, solid fibers are collected in a nonwoven mat. The basic electrospinning setup has three major components: a high-voltage power supply, a capillary device, and a ground collector. A positive displacement pump forces the polymer out of the capillary. Simultaneously, a high-voltage electric field is applied which generates charges in the pendant drop of the polymer liquid at the nozzle. With increasing electric field, the droplet takes on a conical shape (called a Taylor cone), and from its apex a fine liquid jet ejects toward the collector. The electrified jet undergoes stretching and whipping, resulting in a long and thin fiber. As the liquid jet is continuously extended and the solvent evaporates, there is a significant reduction in the diameter of the jet from several hundred micrometers to as low as tens of nanometers.

Eventually, the charged fiber is deposited onto the grounded collector plate as a random, nonwoven mat of nanofibers. Despite the simplicity of the electrospinning setup, the actual mechanism of nanofiber formation is rather complex. The electrospinning process is affected by solution properties such as the type and conformation of the polymer, viscosity, electrical conductivity, and surface tension as well as operating conditions such as the applied voltage, the tip to target distance, and the feed rate of the polymer.<sup>9,10</sup>

Water-insoluble electrospun PVA membranes are often produced in a two-step process: first, an aqueous PVA solution is electrospun to generate nanofibrous membranes, and then the membranes are cross-linked *ex situ* by exposure to GA and a strong acid in solution with a nonsolvent for PVA such as acetone or ethanol. Another approach that has been investigated is vapor phase cross-linking wherein the membranes are exposed to GA and strong acid vapors.<sup>8,17–19</sup> While it is desirable to eliminate post-electrospinning treatment and accelerate the production process, very limited work has been done in trying to cross-link PVA or other nanofibers in a simple one-step process. Recently, single step formation of cross-linked electrospun nanofibers using the basic electrospinning setup with PVA cross-linked with maleic anhydride in the presence of a strong acid and chitosan cross-linked with glutaraldehyde have been examined.<sup>20,21</sup> Changes in viscosity were not observed in the case of chitosan and glutaraldehyde or noted in the case of PVA and maleic anhydride whereas GA is known to cause significant rheological changes when added to PVA solutions.<sup>21,22</sup> The morphology of the electrospun cross-linked material after soaking in an aqueous environment was also not reported; thus, uncertainty remains regarding the effect of soaking on fiber morphology. These results taken together indicate that several issues still remain in understanding fully a single step cross-linking process with electrospinning.

In this study, we undertake a systematic approach to develop and examine an *in situ* process to electrospin cross-linked

\*Corresponding author: e-mail khan@eos.ncsu.edu; Ph 919-515-4519.

nanofibers using a simple setup without reverting to any modifications. We seek to examine the role of rheology as well as the cross-linking reaction in establishing a window for electrospinnability, the effect of cross-linking on final fiber morphology, and whether cross-linking can be exploited to obtain defect-free fibers at entanglement concentrations lower than that typically required.<sup>23,24</sup> Our work builds on the rheology background of our group<sup>25–28</sup> and on the cross-linking work that has been undertaken thus far in the literature on electrospun nanofibers.

Several single step processes for cross-linking electrospun nanofibrous membranes have been reported, eliminating post-electrospinning treatment and accelerating the production process.<sup>20</sup> However, these studies have typically required changes in setup design. *In situ* photo-cross-linking of polymer fibers during electrospinning by incorporating a source of ultraviolet light into the basic electrospinning setup has been reported.<sup>29,30</sup> However, this approach is limited to electrospinnable, photocurable materials and requires a specialized electrospinning setup. A coaxial reactive cross-linking setup, in which the polymer to be cross-linked is in a core syringe and the chemical cross-linking agent is in the shell with an electrospinnable polymer, has also been developed.<sup>31</sup> This methodology, though, requires a second step in which the electrospinnable polymer shell is selectively removed after electrospinning.<sup>31</sup> Using the basic electrospinning setup, chemical cross-linkers have been incorporated into the electrospinning solution but require post-electrospinning treatment to activate the reaction.<sup>31,32</sup>

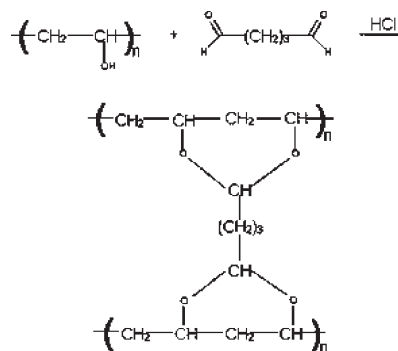
*In situ* cross-linking has also been reported as part of a sol–gel electrospinning process used to generate gelatin and siloxane hybrid nanofibers.<sup>33</sup> The process required aging at 37 °C for 10–30 h prior to electrospinning.<sup>33</sup> The hybrid fibers do not dissolve when immersed in an aqueous environment, but the fiber morphology is not maintained. Sol–gel electrospinning using PVA to form inorganic–organic composite material has been previously described, but in the context of producing inorganic nanofibrous materials such as silica, hydroxyapatite, CeO<sub>2</sub>, etc., following a calcination step.<sup>34–39</sup>

We report a single step process to produce cross-linked PVA nanofibrous membranes using a basic electrospinning setup by incorporating GA and a strong acid (HCl) into the electrospinning solution immediately before processing. The effects of the cross-linking reaction on the rheological properties of the PVA/H<sub>2</sub>O/GA/HCl solution were monitored in parallel with the electrospinning process. Viscosity, elastic modulus, and viscous modulus of the solutions increase as a function of time; however, the values of such parameters are specific for a given solution as they depend on the concentration of the components. Although solution viscosity can be used to predict morphology of electrospun material,<sup>23,24,40</sup> changes in the viscosity were not a convenient parameter to monitor the *in situ* cross-linking process because they are affected by PVA, GA, and HCl concentrations. Changes in the phase angle  $\delta$ , a measure of the ratio of the viscous modulus to the elastic modulus, were not dependent on the concentration of the components; it decreased from  $\sim 90^\circ$  and  $\sim 10^\circ$  universally during cross-linking. Furthermore, the phase angle was a universal parameter that correlated with changes in the morphology of electrospun material. While monitoring changes in the phase angle in parallel with the electrospinning process, we were able to identify appropriate electrospinning windows for PVA/H<sub>2</sub>O/GA/HCl solutions to generate bead-free fibers. The range of the electrospinning windows was determined and could be manipulated by varying the GA and HCl concentrations. Fiber morphology after exposing the electrospun *in situ* cross-linked fibers to aqueous media was also examined.

## Experimental Section

**Materials.** PVA (average molecular weight 127 000 g/mol, 88% hydrolyzed) and hydrochloric acid (37% purity) were

Scheme 1. PVA and GA Cross-Linking Mechanism<sup>7</sup>



obtained from Aldrich. Glutaraldehyde (50% aq) was received from Acros. All materials were used as received.

**Electrospinning.** Aqueous PVA solutions were prepared by stirring mixtures of PVA and deionized water at 60 °C until they were homogeneous. The polymer solution, GA, and HCl were combined in appropriate proportions at room temperature and stirred briefly; a portion of the solution was electrospun and another portion tested rheologically immediately after preparation. The addition of the final component (HCl) was assumed to initiate the cross-linking reaction (Scheme 1).

To electrospin,  $\sim 1$  mL of the PVA/H<sub>2</sub>O/GA/HCl solution was loaded into a syringe fitted with a stainless steel needle (0.508 mm i.d.) and attached to a power supply (Gamma High Voltage Research, D-ES-30PN/M692). A flow rate of 0.5 mL/h, collecting distance of 15 cm between the tip of the needle and the ground collector plate covered with foil, and applied voltage of 10–22 kV were used. To monitor the fiber morphology during the electrospinning process, we conducted rheology on the electrospinning solution and measured the phase angle ( $\delta$ ) as a function of time. We divided the range of  $\delta$  (between 90 and 10) at selected intervals of  $\delta$  (e.g., 75, 45, etc.) and examined the fiber structure at the end of the interval by collecting the fibers on foil until a given  $\delta$  and then changing the foil. Since SEM analysis is limited to the surface, we assumed that the fibers observed corresponded to the  $\delta$  value at the end of the interval although there were fibers lying beneath that were collected over a range of  $\delta$  values. The procedure was repeated for each sample to ensure reproducibility.

In order to determine whether the electrospun material had been cross-linked, small sections of the electrospun mat were cut out at various times and soaked in deionized water at room temperature overnight. Samples were removed from the water and dried at ambient conditions for several hours before further analysis.

**Rheological Measurements.** The zero-shear viscosity of pure PVA solutions was measured at 25 °C using a TA Instruments AR-G2 rheometer using a 40 mm diameter, 2° cone and plate geometry. Dynamic oscillatory shear experiments were also performed on selected samples as a function of time at 25 °C using the same rheometer and configuration, but with a solvent trap. A frequency of 10 rad/s and a stress of 1 Pa were used for all experiments because it was within the linear viscoelastic region of the solutions. Measurements of the elastic ( $G'$ ) and viscous ( $G''$ ) modulus along with loss tangent  $\tan \delta (= G''/G')$ , in which  $\delta$  corresponds to the phase shift, were taken every 30–60 s for up to 8 h.

**Sample Characterization.** To examine the fiber morphology, samples, as spun and after soaking, were sputter-coated with a  $\sim 10$  nm layer gold and analyzed with a scanning electron microscope (SEM, FEI XL-30) at 5 kV. The average fiber size and standard deviation were determined by measuring the diameter of 100 fibers using ImageJ software.

Thermal properties of the nanofibrous mats were examined with differential scanning calorimetry (DSC) with TA

Instruments model DSCQ2000. Samples were heated from  $-20$  to  $235$  °C at a rate of  $10$  °C/min under nitrogen. The glass transition temperature was determined from the inflection point of the specific heat capacity of the second scan as has been previously reported.<sup>41,42</sup> Glass transition temperatures were measured in triplicate.

Infrared spectra ( $400$ – $4000$   $\text{cm}^{-1}$ ) of native PVA and cross-linked samples were measured with a Nicolet 6700 FTIR spectroscope (Thermo Electron Corp.). The absorbance peaks for the hydroxyl ( $-\text{OH}$ ) group at  $3315$   $\text{cm}^{-1}$  and the peak at  $1097$   $\text{cm}^{-1}$ , attributed to  $-\text{COC}$  groups, were normalized. The ratio of the peak heights ( $-\text{COC}/-\text{OH}$ ) were compared for native PVA and cross-linked PVA samples.<sup>43</sup>

## Results and Discussion

**Effect of Polymer Concentration.** We begin by investigating the correlation of native PVA solution dynamics with the resulting morphology of the electrospun material (Figures 1 and 2, left column). Figure 1 shows the normalized zero shear viscosity of PVA solutions as a function of polymer concentration. Solution viscosity, a measure of polymer entanglement, can be used to predict the morphology of electrospun material.<sup>23,24,40</sup> Common fiber morphologies, i.e., beaded fibers and uniform fibers, have been correlated with different polymer concentration regions.<sup>24</sup> For our system, below  $2$  wt % PVA, we find that  $\eta_{\text{sp}} \sim c^{1.3}$  (where  $\eta_{\text{sp}}$  is the specific viscosity and  $c$  is the PVA concentration), consistent with the theoretical prediction for semidilute, nonentangled solutions of a neutral polymer in a good solvent.<sup>40,44</sup> Above  $3$  wt % PVA,  $\eta_{\text{sp}} \sim c^{3.8}$ , characteristic of semidilute entangled solutions.<sup>40,44</sup> The entanglement concentration is  $2.5$  wt % PVA, as indicated by the change in slope in the  $\eta_{\text{sp}}$  vs  $c$  plot (Figure 1).<sup>40</sup> As shown in Figure 2 (left column), semidilute nonentangled solutions (region I) produce nonuniform beaded fibrous materials; semidilute, entangled solutions produce beaded fibers with increased uniformity when qualitatively compared to region I (region II); concentrations above  $6$  wt % PVA (critical concentration) produce uniform fibers (region III). The critical concentration to spin PVA only is  $6.0$  wt %, which is  $2.5$  times greater than the entanglement molecular weight of  $2.5$  wt % (Figure 1) and agrees well with previous studies.<sup>23,24</sup>

PVA solutions from the three concentration regimes were subjected to cross-linking during the electrospinning process by adding GA and HCl, and the fiber morphologies obtained are examined in Figure 2 (right column). The solutions in region I transition from nonuniform beaded fibrous materials to beaded fibers with increased uniformity. Interestingly, solutions in region II transition from beaded fibers with increased uniformity to uniform fibers, some with flattened morphology. Finally, solutions in region III transition from uniform fibers to flattened fibers, some as large as a few micrometers in diameter.

*In situ* cross-linking thus causes significant changes in fiber morphology. The transitions from beaded fibers to uniform fibers to flat fibers indicate increased effective molecular entanglement and molecular weight due to the presence of GA. Flat PVA fibers have been previously observed and attributed to high molecular weights.<sup>45</sup> Koski et al. speculated that at high molecular weights relatively wet fibers are flattened on impact when deposited due to reduced solvent evaporation and increased viscosity. Increased viscosity and increased effective molecular weights may indicate intermolecular cross-linking at the concentrations of PVA and GA used, which are higher than previously used to prepare intramolecular cross-linked water-insoluble gels.<sup>7</sup> Because of the apparent increase in molecular entanglement, semidi-

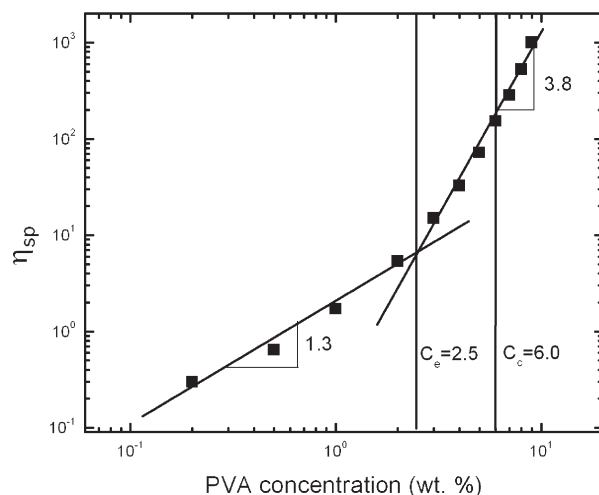


**Figure 1.** Rheological solution properties of PVA: a log–log plot of specific viscosity vs concentration for PVA solutions.

lute entangled PVA solutions (e.g.,  $4\%$  PVA sample in Figure 1 and Figure 2, left) that typically form beaded fibers can now produce relatively uniform fibers during *in situ* cross-linking, thus lowering the critical PVA concentration required for uniform fiber formation.

**Time-Dependent Rheology and Electrospinnability.** The transformation in fiber morphology with time, following the addition of HCl and GA, suggests that significant rheological changes in the precursor solution occur during electrospinning. To examine this issue, dynamic rheological properties of the PVA/ $\text{H}_2\text{O}$ /GA/HCl solutions were monitored as a function of time in parallel with the electrospinning process. Figure 3 shows the complex viscosity, viscous modulus, and elastic modulus for a typical solution undergoing *in situ* cross-linking in the rheometer. We find that PVA with either GA or HCl alone exhibits no time-dependent behavior. However, PVA samples containing both GA and HCl undergo substantial change in rheological behavior with time; the systems start out with  $G'' < G'$  and then become more elastic where  $G' > G''$ . Please note that we did not monitor changes in the frequency spectrum with time using the multiwave technique because it was difficult to find a meaningful frequency–strain combination in the linear regime, and our focus had not been establishing the gel point.<sup>25,46–49</sup> The latter is an interesting issue in terms of its relation to electrospinning with *in situ* cross-linking and will be the subject of a future endeavor.

The viscoelastic changes observed in Figure 3 together with the changes in fiber morphology observed between as spun PVA fibers with and without the addition of GA and HCl (Figure 2) suggest that there are specific windows of time during *in situ* cross-linking in which region II and region III solutions (cf. Figure 2) can successfully electrospin to produce uniform fibers. Measuring the dynamic rheological properties simultaneously with electrospinning, we related the electrospinning window to rheological properties. We use the phase angle ( $\delta$ ) as an indicator of the electrospinning windows for two representative polymer concentrations in the two regimes (Figure 4). As the *in situ* cross-linking progresses,  $\delta$  falls from  $\sim 90^\circ$  to  $\sim 10^\circ$ , indicating a change from a Newtonian solution to a viscoelastic material. The shape of the delta curve (shown with data arbitrarily from  $7$  wt % PVA) is found to be universal for all samples. For a given PVA concentration, production of uniform fibers occurs over a constant range of delta values (“electrospinning window”) that is independent of the concentration

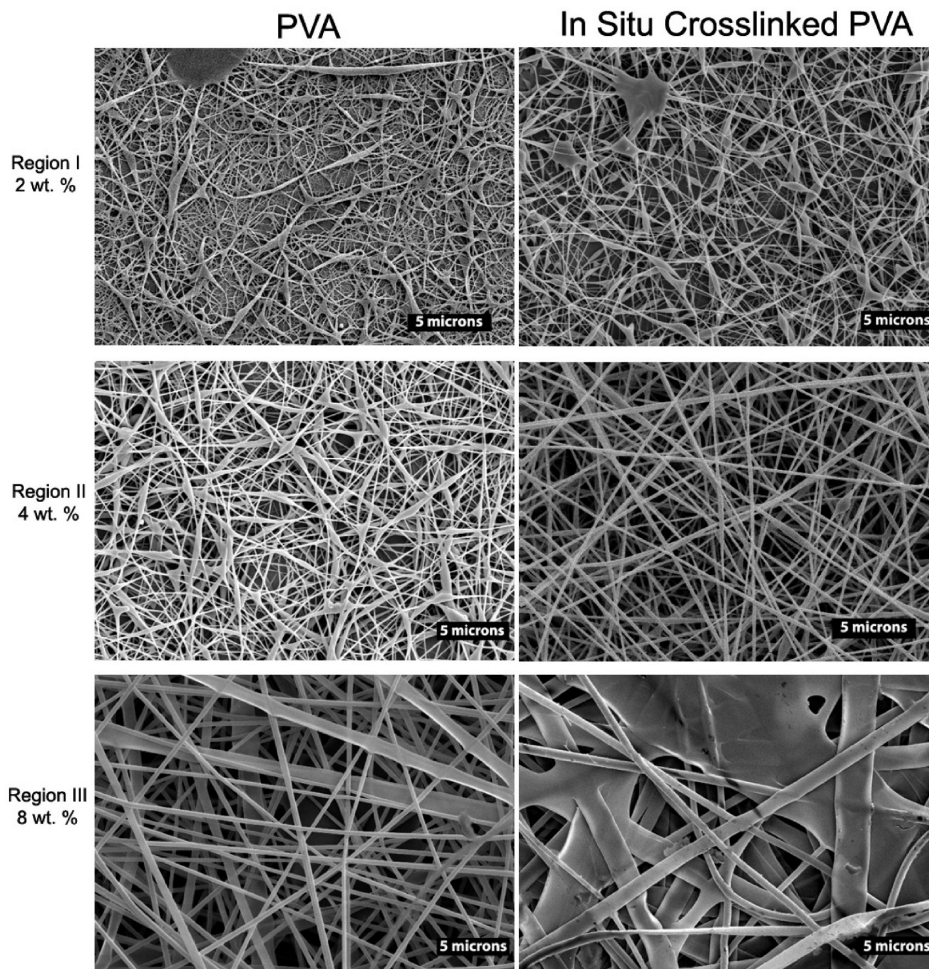


**Figure 2.** SEM micrographs of PVA and *in situ* cross-linked PVA from regions I, II, and III: 2 wt % PVA, 550:1 mol:mol ratio GA:HCl; 4 wt % PVA, 90:1 mol:mol ratio of GA:HCl; 8 wt % PVA, 90:1 mol:mol ratio of GA:HCl.

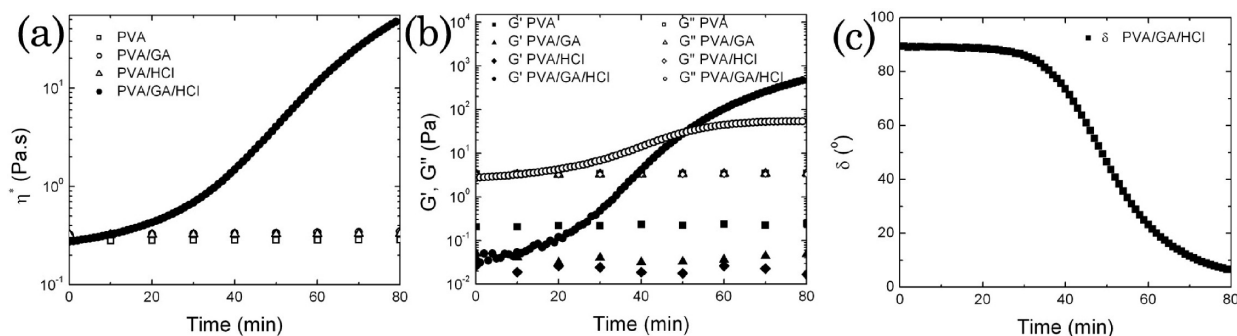


**Figure 3.** Time-dependent rheology of PVA/GA/HCl solutions measured at a frequency of 10 rad/s and stress of 1 Pa. (a) Complex viscosity ( $\eta^*$ ), (b) viscous ( $G''$ ) and elastic ( $G'$ ) moduli, and (c) phase angle ( $\delta$ ) as functions of time during *in situ* cross-linking, shown for a representative sample (7 wt % PVA, 90:1 mol:mol ratio of GA:HCl, 10:1 vol:vol ratio GA:HCl).

of GA or HCl. That is to say, while the time required to reach the critical window and the time span of the electrospinning window changes as functions of GA and HCl concentrations, the values of  $\delta$  that result in an electrospinnable solution remain constant and are a convenient parameter to monitor electrospinnability. For  $\delta >$  electrospinning window, electrospinning results in beaded fibers, while  $\delta <$  the critical window produces flattened fibers.

For example, by comparing the changes in precursor solution rheology to fiber morphology for the region II solution (PVA = 4 wt %), we see that as  $\delta$  falls from 90° to 45°, the number of bead defects decreases. Beaded fibers

give way to fibers when  $\delta$  is  $\sim 25^\circ$  and then to flattened fibers as  $\delta$  drops further to 10°. A conservative estimate for the electrospinning window for region II solutions is for  $45 > \delta > 25$ . For a region III solution (8 wt % PVA), the uniform fibers transition to large flattened fibers as  $\delta$  falls to 75°; thus, a conservative estimate of the electrospinning window for these solutions is  $\delta > 85^\circ$ . In defining an electrospinning window, we examine the fiber morphology at a set of intervals of  $\delta$ ; from this we obtain a range of  $\delta$  values over which high-quality (defect-free) fibers are produced. We allude to this range of  $\delta$  values as electrospinning window and use it as a rough guide to predict electrospinnability of a

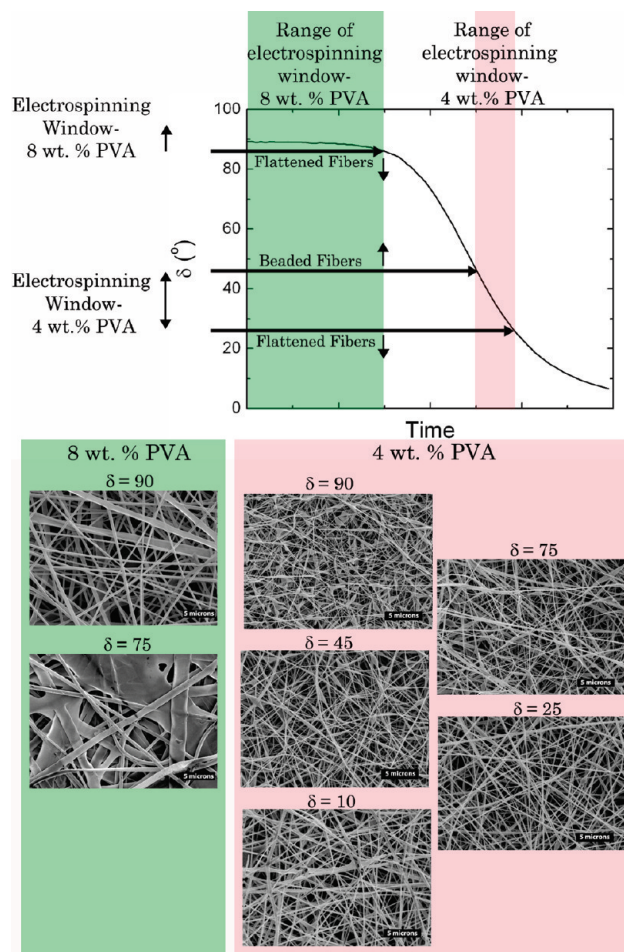


**Figure 4.** Electrospinning window shown in term of  $\delta$  (arrows) for two PVA solutions. The shape of the  $\delta$  curve, from an arbitrary sample, was found to be universal; values of  $\delta$  are used to predict electrospinnability for a given PVA concentration independent of GA and HCl concentrations. The time ranges of the electrospinning window based on the values of  $\delta$  are also shown; however, the time at which the delta values occur are not the same for the two samples.

region II or region III solution, based on the concentration relative to the entanglement concentration.

It is worthwhile to mention that the window to electrospin region II solutions occurs below  $\delta$  values of  $45^\circ$ . Because a  $\delta = 45^\circ$  can be used as a rough estimate of the gel point of a solution, in certain cases *in situ* cross-linking is similar to sol-gel electrospinning.<sup>35,50</sup> Interestingly, in the case of *in situ* cross-linking of PVA through the addition of GA and HCl to the precursor solution produces uniform fibers from solutions of PVA at 1–1.5 times the entanglement concentration, thus lowering the critical electrospinning concentration by 2–2.5-fold. Because lower concentrations of *in situ* cross-linked PVA compared to native PVA can form uniform fibers, smaller PVA fibers can be produced, leading to increased specific surface area.

**Effects of Cross-Linker (GA) and Catalyst (HCl).** Because the kinetics of the cross-linking reaction is known to be a function of polymer, cross-linker, and catalyst concentrations,<sup>5</sup> we manipulated the time range of the electrospinning windows by varying the cross-linker (GA) as well as the catalyst (HCl) concentrations for a constant PVA concentration (region III). By changing the mole to mole ratio of GA to PVA from 54:1 to 181:1, while holding the volume to volume ratio of HCl to GA constant (1:10), the window for region III could be varied from 92 to 9.5 min (Figure 5a).

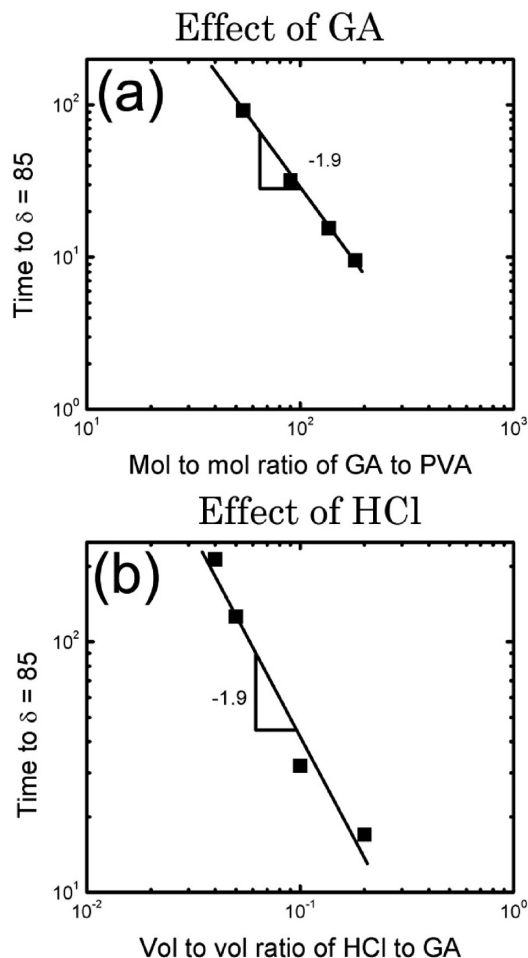


**Figure 5.** Manipulation of the electrospinning window: log–log plots of the range of the electrospinning window vs GA concentration and HCl concentration for solutions above the critical concentration required to electrospin PVA only (region III).

By changing the volume to volume ratio of HCl to GA from 0.04 to 0.2 while holding the mole to mole ratio of GA to PVA constant (90:1), the electrospinning window for region III solution ranged between 210 and 17 min (Figure 5b). Note that the  $\delta$  range is same for all cases as it set by the polymer concentration.

When we change the HCl concentration only while holding all other concentrations constant by changing the volume to volume ratio of HCl:GA while holding the mole to mole ratio of the GA:PVA constant, the range of the electrospinning window is inversely proportional to the square of the HCl concentration (Figure 5b). However, when the mole to mole ratio of GA:PVA is varied while holding the volume to volume ratio of HCl:GA constant, both concentrations of GA and HCl are changing. In the case where the catalyst (HCl) and the cross-linker (GA) concentrations are both changing (Figure 5a), we observe that the scaling of the electrospinning window remains approximately the same ( $-2$ ) as the case where only the HCl concentration was changed. These data imply that the range of the electrospinning window has little dependence on GA concentration but changes with the square of the HCl concentration. The result is similar to previous studies that examined the kinetics of the cross-linking reaction between GA and PVA using  $\text{H}_2\text{SO}_4$  as a catalyst in a solution cast film where Kim et al. report a first-order dependence on  $\text{H}_2\text{SO}_4$  concentration. The authors also report a first-order dependence on GA

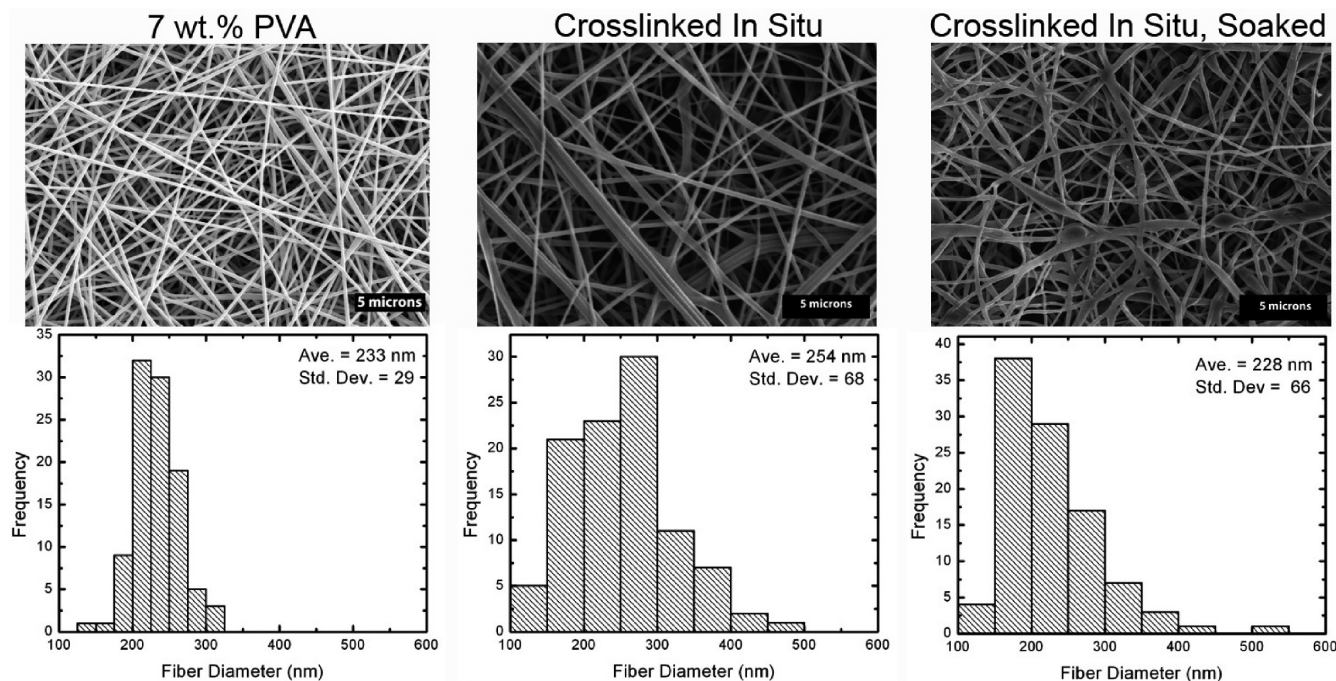


**Figure 6.** SEM micrographs and fiber size distributions of PVA, *in situ* cross-linked PVA, and *in situ* cross-linked PVA, soaked in water (7 wt % PVA, 90:1 mol:mol ratio GA:HCl, 10:1 vol:vol ratio GA:HCl determined by measuring 100 fibers).

concentration, whereas we see an approximate zero-order dependence when using the range of the electrospinning window as a measure of reaction kinetics.<sup>5</sup> This result indicates that the *in situ* cross-linking reaction is done with a large excess of GA; therefore, the reaction kinetics are not strong functions of GA concentration at the levels used. Although there is some arbitrariness in the choice of  $\delta$ , our results show that for a chosen window the time range can be manipulated using the kinetics.

**Effect of Soaking on Fiber Morphology.** Maintaining the fiber morphology is important for applications where high surface area-to-mass ratios are considered advantageous. In specific cases, we were able to successfully cross-link PVA during the electrospinning process, as the fiber morphology could be maintained after soaking in water. This is illustrated for a sample containing 7 wt % PVA in Figure 6. The average fiber diameter is not affected by *in situ* cross-linking PVA ( $254 \pm 68$  nm) compared to native PVA ( $233 \pm 29$  nm). Further, the size is not significantly affected by soaking in water ( $228 \pm 66$  nm). We speculate that the *in situ* cross-linked fibers show a wider distribution, indicated by the increased standard deviation, due to the constantly changing viscosity of the electrospinning sample. The *in situ* cross-linked PVA also had a glass transition temperature of  $85.3 \pm 0.9$  °C (average of three measurements  $\pm$  standard deviation), higher than electrospun samples of PVA only with a glass transition temperature of  $70.2 \pm 0.5$  °C (data not shown but included as Supporting Information). The change in glass transition temperature is comparable to previous reports for cross-linked PVA.<sup>41</sup> FTIR analyses of the cross-linked sample (data not shown but included as Supporting Information) shows a decrease in absorbance at  $\sim 3315$   $\text{cm}^{-1}$  relative to the absorbance at  $\sim 1097$   $\text{cm}^{-1}$  due to the cross-linking reaction in which the hydroxyl groups react with aldehyde groups to form ether linkages.<sup>42,43</sup> The ratio of the peak height of the absorbance at  $\sim 1097$   $\text{cm}^{-1}$  to the absorbance at  $\sim 3315$   $\text{cm}^{-1}$  for the cross-linked sample is  $\sim 17\%$  higher than the native PVA sample, further evidence of the *in situ* cross-linking reaction.

We observed that the morphology after soaking was affected by the GA and HCl concentrations in the electrospinning solution. Examining 7 wt % PVA solutions (region III), there were critical GA and HCl concentrations required to maintain fiber morphology after soaking in water. SEM images of 7 wt % PVA with a 10:1 volume of GA to volume of HCl, with various concentrations of GA before and after soaking are shown in Figure 7. Below a mole of GA to mole of PVA ratio of 27:1, all electrospun material dissolves when soaked in water. Between a ratio of 36:1 and 90:1, the PVA is cross-linked, but the fibers fuse when soaked in water and the fiber morphology is not maintained. At a ratio of 90:1, the fiber morphology is maintained after soaking in water, but above a ratio of 90:1 some swelling occurs.

SEM images of 7 wt % PVA with a 90:1 mole GA to mole PVA ratio, with various concentrations of HCl before and after soaking, are shown in Figure 8. Below a volume GA to volume of HCl ratio of 50:1, the PVA was not affected by the addition of GA within the time frame examined and was not cross-linked, and thus the electrospun material dissolved when soaked in water. Above a ratio of 25:1 but below 10:1, the PVA cross-linked but the fiber morphology was not maintained after soaking in water. With a ratio of 10:1, the PVA was successfully cross-linked and the fiber morphology was maintained after soaking in water. While the PVA cross-linked with ratios above 10:1, the fibers swelled significantly when soaked in water.

The effective molecular weight of PVA increases due to changes in the effective polymer entanglement arising from intermolecular cross-linking during the electrospinning process, leading to larger fibers with flattened morphology. However, flattened fibers do not appear to cross-link consistently, which suggests there may be an upper limit to the fiber size and molecular weight that can be cross-linked *in situ*. Above the critical GA and HCl concentration, the onset of the flattened fiber morphology due to the increase in entanglement, and thus polymer molecular weight occurs quickly relative to the time it takes to sufficiently cross-link the electrospun fibers. The resulting fibers thus lose their

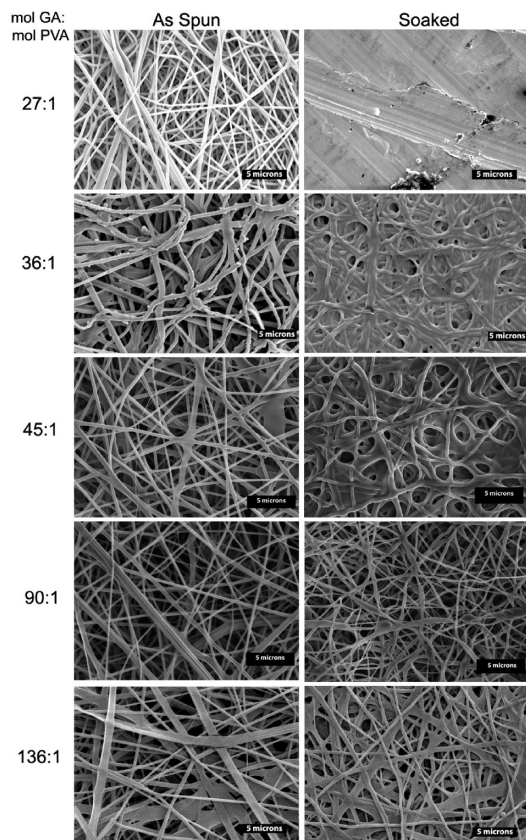


**Figure 7.** SEM micrographs of *in situ* cross-linked PVA with varying GA concentration before and after soaking in water.

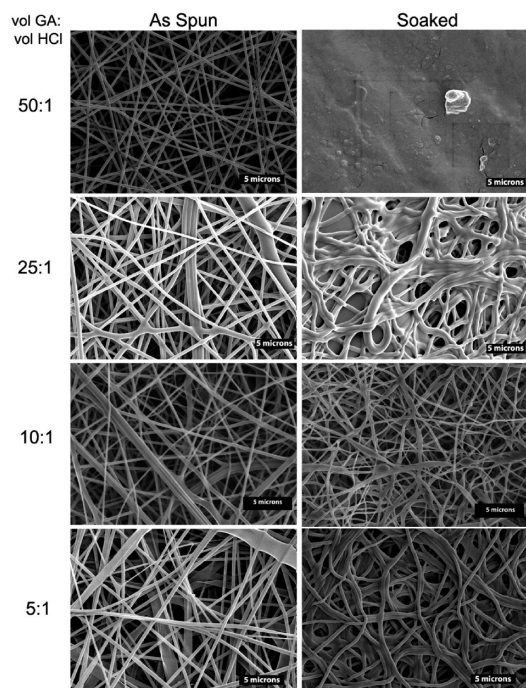


**Figure 8.** SEM micrographs of *in situ* cross-linked PVA with varying GA concentration before and after soaking in water.

morphology when exposed to water. However, at the critical GA and HCl concentrations, in the range of the electrospinning window, there is a fine balance between increasing molecular weight and entanglement of PVA and sufficient cross-linking to maintain fiber morphology.

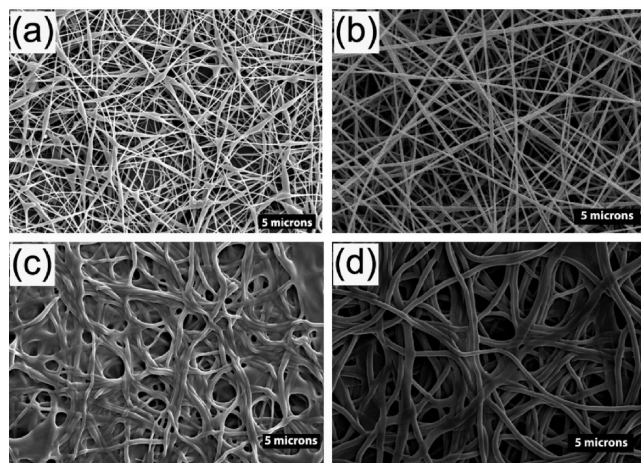


**Figure 9.** SEM micrographs of (A) 4 wt % PVA (region II), (B) *in situ* cross-linked 4 wt % PVA when  $\delta$  was 25, (C) 4 wt % PVA with a mole PVA to mole GA ratio of 90:1 *in situ* cross-linked and soaked, and (D) 4 wt % PVA with a mole to mole PVA to mole GA ratio of 180:1 *in situ* cross-linked and soaked.

Electrospun fibers from region II were also examined before and after soaking (Figure 9) and a mole PVA to mole GA ratio of 90:1 was not sufficient to successfully cross-link the PVA so that the fiber morphology was maintained in water. With higher concentration of GA, the fiber morphology after soaking could be improved but not maintained as the fibers swell significantly after soaking in water (Figure 9). It appears that in the time it takes to electrospin the GA present in region II solutions cross-linked *in situ* is only sufficient to increase entanglement to eliminate beads and allow for production of uniform fibers. However, the GA present is not sufficient to successfully cross-link those fibers such that the fiber morphology is maintained after soaking in water.

Because lower concentrations of *in situ* cross-linked PVA compared to PVA can form uniform fibers, smaller PVA fibers can be produced. For example, 7 wt % pure PVA (region III) has an average fiber diameter of  $233 \pm 29$  nm, whereas 4 wt % pure PVA (region II) forms beaded fibers. When 4 wt % PVA is cross-linked *in situ*, at the end of the electrospinning window, the average fiber diameter is  $178 \pm 29$  nm. The 25% reduction in fiber diameter increases specific surface area by 33%. The smaller *in situ* cross-linked 4 wt % PVA would have to be further cross-linked in a post-electrospinning step to maintain fiber morphology when soaked in water.

## Conclusions

We have incorporated a chemical cross-linker and catalyst to PVA solutions to perform *in situ* cross-linking of nanofibers with a basic electrospinning setup. The cross-linking reaction causes significant changes in solution rheology and fiber morphology. As the solution viscosity increases, molecular entanglement increases as fibers can transition from beaded fibers to uniform fibers to flat fibers. The window for obtaining uniform fibers was identified by simultaneously measuring dynamic rheological properties and electrospinning, and the range of the window could be manipulated by varying the molar ratio of PVA to GA and the volume ratio of GA to HCl. The transition from beaded fibers to uniform fibers lowers the critical PVA concentration required to electrospin from 2 to 2.5 times the entanglement concentration for PVA solutions to  $\sim 1$ –1.5 times the entanglement concentration for PVA/H<sub>2</sub>O/GA/HCl solutions. *In situ* cross-linking also yields insoluble fibers whose morphology can

be maintained after soaking in water. Critical GA and HCl concentrations were observed for cross-linking and maintaining fiber morphology.

**Acknowledgment.** This work was supported by the STC program of the U.S. National Science Foundation under Agreement CHE-9876674 and the U.S. Department of Education Graduate Assistance in Areas of National Need (GAANN) Fellowship Program at North Carolina State University. The authors thank Dr. Jan Genzer and A. E. Ozcam for their assistance with FTIR measurements and S. A. Arvidson for discussions and her assistance with thermal analysis.

**Supporting Information Available:** DSC scans and FTIR spectra. This material is available free of charge via the Internet at <http://pubs.acs.org>.

## References and Notes

- Zhang, C.; Yuan, X.; Wu, L.; Sheng, J. *Eur. Polym. J.* **2005**, *41*, 423–432.
- Wang, X.; Fang, D.; Yoon, K.; Hsiao, B. S.; Chu, B. *J. Membr. Sci.* **2006**, *278*, 261–268.
- Ding, B.; Kim, H.; Lee, S.; Shao, C.; Lee, D.; Park, S.; Kwang, G.; Choi, K. *J. Polym. Sci., Polym. Lett.* **2002**, *40*, 1261–1268.
- Yeom, C.; Lee, K. *J. Membr. Sci.* **1996**, *109*, 257–265.
- Kim, K.; Lee, S.; Han, N. *Korean J. Chem. Eng.* **1994**, *11*, 41–47.
- Praptowidodo, V. S. *J. Mol. Struct.* **2005**, *739*, 207–212.
- Brasch, U.; Burchard, W. *Macromol. Chem. Phys.* **1996**, *197*, 223–235.
- Wang, X.; Chen, X.; Yoon, K.; Fang, D.; Hsiao, B. S.; Chu, B. *Environ. Sci. Technol.* **2005**, *39*, 7684–7691.
- Burger, C.; Hsiao, B. S.; Chu, B. *Annu. Rev. Mater. Res.* **2006**, *36*, 333–368.
- Li, D.; Xia, Y. *Adv. Mater.* **2004**, *16*, 1151–1170.
- Reneker, D. H.; Chun, I. *Nanotechnology* **1996**, *7*, 216–223.
- Huang, Z.; Zhang, Y. Z.; Kotaki, M.; Ramakrishna, S. *Compos. Sci. Technol.* **2003**, *63*, 2223–2253.
- Fridrikh, S. V.; Yu, J. H.; Brenner, M. P.; Rutledge, G. C.; et al. *Phys. Rev. Lett.* **2003**, *90*, 144502-1–4.
- Saquin, C.; Manasco, J. L.; Khan, S. A. *Small* **2009**, *5*, 944–951.
- Gupta, A.; Saquin, C. D.; Afshari, M.; Tonelli, A. E.; Khan, S. A.; Kotek, R. *Macromolecules* **2009**, *42*, 709–715.
- Talwar, S.; Hinestroza, J.; Pourdehimi, B.; Khan, S. A. *Macromolecules* **2008**, *41*, 4275–4283.
- Wang, Y.; Hsieh, Y. L. *J. Membr. Sci.* **2008**, *309*, 73–81.
- Wu, L.; Yuan, X.; Sheng, J. *J. Membr. Sci.* **2005**, *250*, 167–173.
- Taepaiboon, P.; U. Rungsardthong, U.; Supaphol, P. *Nanotechnology* **2007**, *18*, 175102.
- Schiffman, J. D.; Schauer, C. L. *Biomacromolecules* **2007**, *8*, 2665–2667.
- Yang, E.; Qin, X.; Wang, S. *Mater. Lett.* **2008**, *62*, 3555–3557.
- Kjoniksen, A.; Nystrom, B. *Macromolecules* **1996**, *29*, 5215–5222.
- Shenoy, S. L.; Bates, W. D.; Frisch, H. L.; Wnek, G. E. *Polymer* **2005**, *46*, 3372–3384.
- McKee, M. G.; Wilkes, G. L.; Colby, R. H.; Long, T. E. *Macromolecules* **2004**, *37*, 1760–1767.
- Chiou, B.; English, R. J.; Khan, S. A. *Macromolecules* **1996**, *29*, 5368–5374.
- Chiou, B.; Khan, S. A. *Macromolecules* **1997**, *30*, 7322–7328.
- Walls, H. J.; Caines, S. B.; Sanchez, A. M.; Khan, S. A. *J. Rheol.* **2003**, *47*, 847–868.
- Talwar, S.; Harding, J. R.; Oleson, K. R.; Khan, S. A. *Langmuir* **2009**, *25*, 794–802.
- Gupta, P.; Trenor, S. R.; Long, T. E.; Wilkes, G. L. *Macromolecules* **2004**, *37*, 9211–9218.
- Kim, S.; Kim, S. H.; Nair, S.; Moore, E. *Macromolecules* **2005**, *38*, 3719–3723.
- Ji, Y.; Ghosh, K.; Li, B.; Sokolov, J. C.; Clark, R. A. F.; Rafailovich, M. H. *Macromol. Biosci.* **2006**, *6*, 811–817.
- Liu, H.; Zhen, M.; Wu, R. *Macromol. Chem. Phys.* **2007**, *208*, 874–880.
- Song, J.; Yoon, B. H.; Kim, H. E.; Kim, H. W. *J. Biomed. Mater. Res. A* **2008**, *84a*, 875–884.
- Shao, C.; Kim, H.; Gong, J.; Ding, B.; Lee, D.; Park, S. *Mater. Lett.* **2003**, *57*, 1579–1584.
- Shao, C.; Kim, H.; Geng, J.; Lee, D. *Nanotechnology* **2002**, *13*, 635–637.
- Dai, X.; Shivkumar, S. *J. Am. Ceram. Soc.* **2007**, *90*, 1412–1419.
- Yang, X.; Shao, C.; Liu, Y.; Mu, R.; Guan, H. *Thin Solid Films* **2005**, *478*, 228–231.
- Yu, N.; Shao, C.; Liu, Y.; Guan, H.; Yang, X. *J. Colloid Interface Sci.* **2005**, *285*, 163–166.
- Shao, C.; Guan, H.; Liu, Y.; Gong, J.; Yu, N.; Yang, X. *J. Cryst. Growth* **2004**, *267*, 380–384.
- Klossner, R. R.; Queen, H. A.; Coughlin, A. J.; Krause, W. E. *Biomacromolecules* **2008**, *9*, 2947–2953.
- Krumova, M.; Lopez, D.; Benavente, R.; Mijangos, C.; Perena, J. M. *Polymer* **2000**, *41*, 9265–9272.
- Hasimi, A.; Stravropoulou, A.; Papadokostaki, K. G.; Sanopoulou, M. *Eur. Polym. J.* **2008**, *44*, 4098–4107.
- Hyder, M. N.; Huang, R. Y. M.; Chen, P. *J. Membr. Sci.* **2006**, *283*, 281–290.
- Dobrynin, A. V.; Colby, R. H.; Rubinstein, M. *Macromolecules* **1995**, *28*, 1856–1871.
- Koski, A.; Yim, K.; Shivkumar, S. *Mater. Lett.* **2004**, *58*, 493–497.
- Winters, H. H.; Chambon, F. *J. Rheol.* **1986**, *30*, 367–382.
- Holly, E. E.; Venkataraman, S. K.; Chambon, F.; Winters, H. H. *J. Non-Newtonian Fluid Mech.* **1988**, *27*, 17–26.
- Chiou, B.; Raghavan, S. R.; Khan, S. A. *Macromolecules* **2001**, *34*, 4526–4533.
- Raghavan, S. R.; Chen, L. A.; McDowell, C.; Khan, S. A. *Polymer* **1996**, *37*, 5869–5875.
- Li, D.; Xia, Y. *Nano Lett.* **2004**, *3*, 555–560.